

Mechanical and biological properties of hydroxyapatite reinforced with 40 vol. % titanium particles for use as hard tissue replacement

CHENGLIN CHU*

Department of Mechanical Engineering, Southeast University, Nanjing 210018, China
E-mail: clchu@seu.edu.cn

XIAOYAN XUE

General Medicine Centre, Zhong Da Hospital, Southeast University, Nanjing 210009, China

JINGCHUAN ZHU, ZHONGDA YIN

School of Materials Science and Engineering, Harbin Institute of Technology, Box 433, Harbin 150001, China

Hydroxyapatite (HA)-based composite reinforced with 40 vol. % Ti particles was fabricated by the optimal technical condition of hot pressing technique. The mechanical and biological properties of the composite were studied by mechanical and *in vivo* methods. The experimental results show that HA and Ti phases are the predominant phases of the composite with partially decomposition of HA phase into α - $\text{Ca}_3(\text{PO}_4)_2$ and $\text{Ca}_4\text{O}(\text{PO}_4)_2$. Comparing with HA–20 vol. % Ti composite manufactured under the same conditions, HA–40 vol. % Ti composite with similar elastic modulus (79.3 GPa) and Vicker's hardness (2.94 GPa) has a higher bending strength (92.1 MPa). Moreover, fracture toughness of HA–40 vol. % Ti composite with crack bridging as the chief toughening mechanisms can reach 2.692 MPa m^{-1} , which can meet the basic toughness demand of the replaced hard tissues for heavy load-bearing applications. Work of fracture of HA–40 vol. % Ti composite is 91.2 J m^2 , which is 22.9 times that of pure HA ceramic and even 2.4 times that of Al_2O_3 bioceramic. The results of *in vivo* studies show HA–40 vol. % Ti composite has excellent biocompatibility and could integrate with bone. In the early stage after the implantation of the samples, the osteointegration ability of the composite is better than that of pure titanium.

© 2004 Kluwer Academic Press

1. Introduction

As reviewed by Hench [1], Williams [2], Suchanek and Yoshimura [3], hydroxyapatite (HA) is the main inorganic constituent of hard tissues and has excellent biocompatibility. However, pure HA ceramic with poor mechanical properties is not suitable for load-bearing applications. The ideal biomaterials for hard tissue replacement may be acquired by the preparation of HA ceramic composites. Polyethylene (PE)–HA composite with the mechanical properties similar to those of bones developed by Bonfield [4] is a very good example. Until now, many reinforcements, including particles [5], whiskers [6] and long fibers [7] have been used in HA ceramic to improve its mechanical reliability. Although significant toughening effect has been reported for whisker-reinforced HA-based composites [3], many commercially available whiskers are considered as potentially carcinogenic materials according to the so-called Stanton and Pott criterion [8, 9]. Some bioinert metals and ceramics have been used as particle

reinforcements [10–16]. Titanium metal is the preferred particle reinforcement with the significant toughening effect by energy-absorbing mechanism due to the plastic deformation of ductile metal particles at the tips of cracks [10, 11] and the good biocompatibility [17, 18].

The investigations on fabrication and characterization of HA–20 vol. % Ti composite have been reported [19]. It could be found that fracture toughness of HA-based composite reinforced with 20 vol. % Ti particles is up to 1 MPa m^{-1} , while that of pure HA produced in the same way is only 0.663 MPa m^{-1} . However, the fracture toughness of a compact human bone for heavy load-bearing applications may reach above 2 MPa m^{-1} , thus HA–20 vol. % Ti composite cannot be used for such hard tissue replacement. In this paper, in order to improve its mechanical properties further, HA-based composite reinforced with 40 vol. % Ti particles was fabricated by hot-pressing technique based on our previous work [19]. The mechanical and biological properties of the composite were studied by mechanical and *in vivo* methods.

*Author to whom all correspondence should be addressed.

2. Experimental procedure

2.1. Raw materials and fabrication of the composite

Hydroxyapatite powders used in this paper were prepared by the reaction between $\text{Ca}(\text{NO}_3)_2$ and $(\text{NH}_4)_2\text{HPO}_4$. Its Ca/P ratio was $1.67 \pm 2.0\%$ and the content of heavy metals, such as Pb, As, Hg and Cd is less than 1.0 ppm. The chemical composition of titanium powders used was (wt %): Ti 99.3, Fe 0.039, O 0.35, N 0.035, C 0.025, Cl 0.034, H 0.024 and Si 0.0018. Ti particles had an average size of $45.2 \mu\text{m}$, while the average size of HA particles is $1.75 \mu\text{m}$. The mixed powders of HA and Ti with 40% Ti in volume fraction were first blended by ball milling for 24 h and then compacted at 200 MPa. Finally, green compacts were hot-pressed at 1100°C under a pressure of 20 MPa in nitrogen atmosphere for 30 min with a heating rate of $10^\circ\text{C}/\text{min}$ and a cooling rate of $6^\circ\text{C}/\text{min}$. The pure Ti samples in contrast with the composite were also produced in the same way.

2.2. Characterization

The phase constitution was analyzed by X-ray diffraction (XRD). The density of sintered samples was measured accurately using distilled water by Archimedes method. The relative density was calculated using the measured density divided by the theoretical one. Vickers' hardness was tested on polished surfaces under a load of 98 N. Three-point bending tests were performed on Instron-testing machine (1186 type) to determine elastic modulus, bending strength and fracture toughness. Samples for microstructure observations were cut with a diamond saw, and their surfaces were ground and polished. The fracture surfaces of the samples were covered with a thin film of gold by vacuum-deposition and then examined by scanning electron microscope (SEM).

2.3. In vivo study

2.3.1. Implant preparation and surgical operation

As shown in Fig. 1(a), HA-40 vol. % Ti composite and pure Ti metal were cut into rectangular specimens about $3.3 \text{ mm} \times 3.3 \text{ mm} \times 5\text{--}6 \text{ mm}$ in dimension using a diamond saw. The cross-sectional view of the predrilled

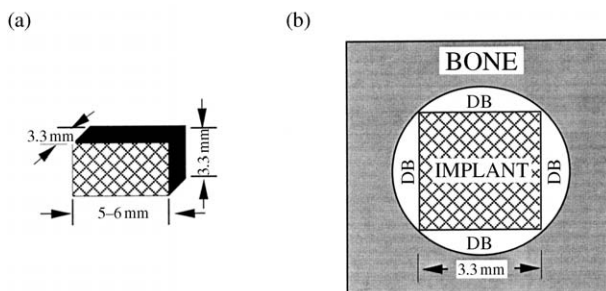


Figure 1 Schematic configuration of the implant model. (a) Rectangular specimen for implantation and (b) cross-sectional view of the predrilled hole with implant in the skull (DB-defective bone region).

hole with implant in the skull of several New Zealand White rabbits of 2.5 kg weight is illustrated in Fig. 1(b). The defective bone (DB) region was designed for bone healing. Before implantation, all implants were cleaned with distilled water and sterilized by autoclaving at 121°C for 30 min. Prophylactic antibiotic was given once during operation. The rectangular implants were inserted into predrilled holes of 4.76 mm diameter using sterile surgical techniques. With implants randomly distributed, each rabbit contained eight implants (four each of HA-40 vol. % Ti composite and pure Ti metal).

2.3.2. Observations of tissues and interfaces between bone and implants

After two, four, eight or 12 weeks, two rabbits were sacrificed and the harvested samples were distributed into two parts. The first part of the harvested samples was fixed in glutaraldehyde, swilled by phosphate buffered saline (PBS), then fixed by osmic acid and swilled by PBS again, finally dehydrated and evaporated at critical point. The treated samples were covered with a thin film of gold by vacuum-deposition and then examined by SEM. The second part of the harvested samples was fixed in 10% buffered formalin. The fixed samples were decalcified in an acid compound (1000 mL solution containing 8.5 g sodium chloride, 100 mL formalin, 70 mL of 37% hydrochloric acid, 80 mL formic acid, 40 g aluminum chloride and 25 mL glacial acetic acid). Dehydrated in alcohol and embedded in paraffin, decalcified sections were stained with hematoxylin and eosin (HE) for light microscopic observation.

3. Results and discussion

3.1. Fabrication and mechanical properties of HA-40 vol. % Ti composite

Based on our previous work [19], the optimal technical condition of hot-pressing technique was chosen to prepare HA-40 vol. % Ti composite. Fig. 2 shows the microstructure of HA-40 vol. % Ti composite, in which the white phase is Ti and the dark one is HA. Obviously Ti metal particles distribute homogeneously in HA ceramic matrix. The phase constitution may play a very important role on the biological properties of the

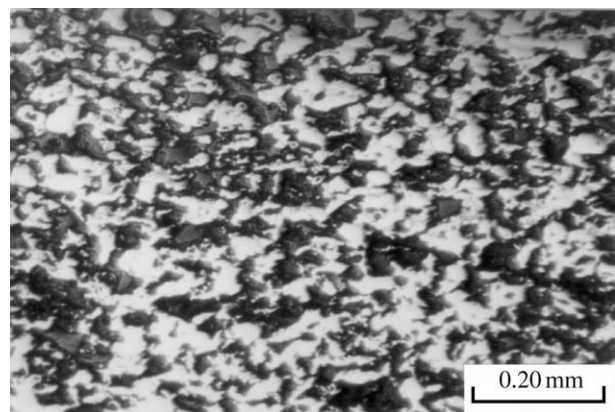


Figure 2 Microstructure of HA-40 vol. % Ti composite, in which the white phase is Ti and the dark one is HA.

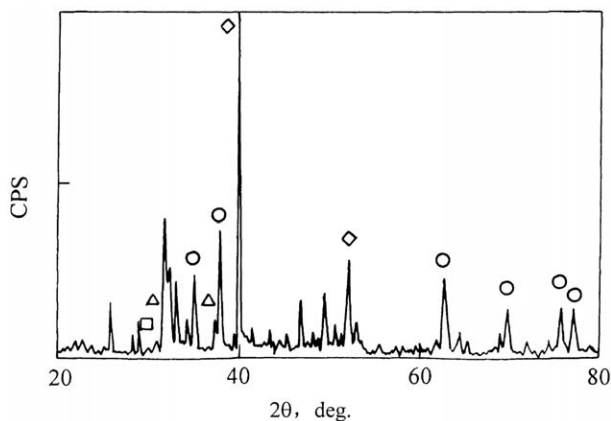


Figure 3 XRD pattern of HA-40 vol. % Ti composite. α -Ca₃(PO₄)₂ (Δ), Ca₄O(PO₄)₂ (\square), Ti (\circ), Ti and HA (\diamond), and HA (unmarked).

composite. Fig. 3 shows the XRD pattern of HA-40 vol. % Ti composite. It could be found that HA and Ti phases are the predominant phases of the composite like HA-20 vol. % Ti composite [19]. In addition, the sintering process at a high temperature resulted in the formation of two second phase, such as α -Ca₃(PO₄)₂ (TCP) and Ca₄O(PO₄)₂. The presence of second phase is the common feature for HA-based composites fabricated by thermal processing because the existence of reinforcements can degrade the structural stability of HA crystal and promote the dehydration and decomposition of HA phase [19].

Table I shows the characteristics of HA-40 vol. % Ti composite. In order to bring into comparison, the characteristics of pure HA ceramic and HA-20 vol. % Ti composite after the literature [19] were also listed in Table I. It could be found that the relative density of HA-40 vol. % Ti composite is 93.3%, while the one of pure HA ceramic can reach 98.2%. Obviously, the sintering ability of HA-Ti composite compacts is inferior to that of pure HA powder compacts. This may be due to the promotion of Ti phase on the decomposition of HA ceramics and the difference of sintering shrinkages between HA particles and Ti ones. It should be pointed out that the decomposition reaction of HA phase with the generation of new phases can block the sintering densification of the materials [20, 21]. By the way, the existence of some pores in the composite can improve the bioactivity of the biomaterials effectively on the premise of the mechanical guarantee [22, 23].

Owing to the low relative density of the composite and the lower hardness of Ti metal comparing with pure HA ceramic, Vicker's hardness of HA-40 vol. % Ti composite is 2.94 GPa, which is lower than that of HA-20 vol. % Ti composite (3.13 GPa) and far lower than that

of pure HA ceramic (4.72 GPa). Like HA-20 vol. % Ti composite, HA-40 vol. % Ti composite has a lower elastic modulus (79.3 GPa) than pure HA (110.9 GPa). The implant with low elastic modulus is preferred to match that of replaced bones (7-25 GPa) [1]. The elastic modulus of the composite could be estimated by the following mixture law:

$$E_{\text{HA-Ti}} = E_{\text{Ti}}(1 - f) + E_{\text{HA}}f \quad (1)$$

where E_{Ti} is elastic modulus of Ti metal (107 GPa) and E_{HA} is elastic modulus of dense HA ceramic (117 GPa). f is the volume fraction of HA ceramic. Because the porosity plays an important role on elastic modulus of the material, the influence of the porosity must be taken into account. The experiential relationship between elastic modulus of HA ceramic sintered and the porosity (p) can be expressed as the following [10]:

$$E_{\text{HA}} = 117(1 - 2.01 p) \quad (2)$$

Therefore, the first expression for elastic modulus of HA-Ti composite can be altered as the following:

$$E_{\text{HA-Ti}} = 107 + (10 - 235 p)f \quad (3)$$

The theoretic values of elastic moduli of HA-40 vol. % Ti composite and HA-20 vol. % Ti composite calculated by the third expression are 103.5 GPa and 96.5 GPa respectively, which are higher than those tested.

Reinforced by Ti particles, bending strength of HA-40 vol. % Ti composite is 92.1 MPa, which is slightly higher than that of HA-20 vol. % Ti composite and about three times that of pure HA ceramic. However, fracture toughness of HA-40 vol. % Ti composite can reach 2.692 MPa m^{-1/2}, which is greatly higher than that of HA-20 vol. % Ti composite (0.987 MPa m^{-1/2}) and about four times that of pure HA ceramic. Moreover, fracture toughness of HA-40 vol. % Ti composite can meet the basic toughness demand of the replaced hard tissues for heavy load-bearing applications. As discussed in the literature [19], work of fracture of the materials (G_{IC}) could be gained by the following expression from fracture toughness (K_{IC}) and elastic modulus (E),

$$G_{\text{IC}} = K_{\text{IC}}^2/E \quad (4)$$

Works of fracture of HA-20 vol. % Ti composite is 12.8 J m⁻², while work of fracture of HA-40 vol. % Ti composite with relatively higher fracture toughness and low elastic modulus can reach 91.2 J m⁻², which is 22.9 times that of pure HA ceramic and even 2.4 times that of Al₂O₃ bioceramic (38 J m⁻²) with $E = 380$ GPa and $K_{\text{IC}} = 3.8$ MPa m^{-1/2}.

Fracture surface characteristics of HA-40 vol. % Ti composite are shown in Fig. 4(a). It could be found that

TABLE I Characteristics of HA-Ti composites and pure HA ceramic

Materials	ρ (g/cm ³)	ρ_{rel} (%)	Porosity (%)	E (GPa)	σ_{bs} (MPa)	K_{IC} (MPa · m ^{1/2})	HV (GPa)
HA-40 vol. % Ti composite	3.499	93.3	6.7	79.3 ± 6.1	92.1 ± 11.1	2.692 ± 0.270	2.94 ± 0.09
HA-20 vol. % Ti composite	3.141	90.2	9.8	75.9 ± 8.7	78.6 ± 9.2	0.987 ± 0.080	3.13 ± 0.21
Pure HA	3.161	98.2	1.8	110.9 ± 10.4	36.9 ± 10.5	0.663 ± 0.100	4.72 ± 0.16

ρ : density of materials sintered by hot-pressing at 1100 °C.

ρ_{rel} : relatively density of materials sintered by hot-press at 1100 °C.

E , σ_{bs} , K_{IC} and HV; Young's modulus, bending strength, fracture toughness and Vickers hardness of materials sintered by hot-pressing at 1100 °C.

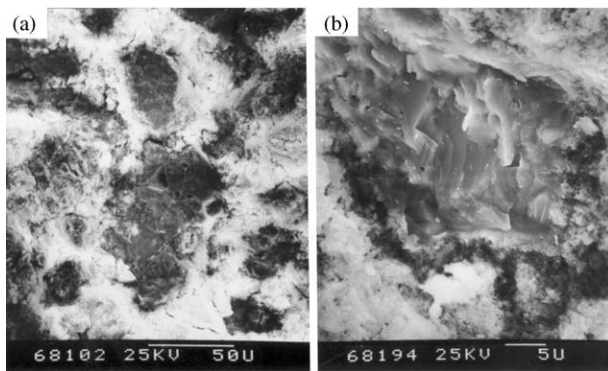


Figure 4 SEM fractographs show fracture surface characteristics of HA-40 vol.% Ti composite. (a) Low magnification and (b) high magnification, from which it could be found that there are some tearing edges on the fracture surfaces of coarse Ti particles and cracks along the interface between Ti and HA phases.

HA matrix presents intergranular fracture without macroscopic plastic deformation, while Ti particles are coarse and appear quasi-cleavage fracture. Detailed examination (Fig. 4(b)) shows that there are some tearing edges on the fracture surfaces of Ti particles and cracks along the interface, which indicates that the toughening mechanism in HA-40 vol.% Ti composite is different from that of HA-20 vol.% Ti composite with crack deflection as the chief toughening mechanism [19]. The presence of many cracks along the interface reveals that the interface bonding is very weak. The cracks may be easily deflected into the matrix and propagate along the interface when encountering Ti particles. It is obvious that crack deflection is one of toughening mechanisms in HA-40 vol.% Ti composite. However, the contribution

of crack deflection to the toughness can be predicted according to a model [24], to be only about 22–35% of the matrix toughness, while the toughness of HA-40 vol.% Ti composite is 4.3 times that of monolithic HA. Thus, crack deflection is not the chief toughening mechanisms for HA-40 vol.% Ti composite. The existence of tearing edges on fracture surfaces of Ti particles shows that the toughening is attributed to crack bridging as an energy-absorbing mechanism at sites of Ti particles. Obviously, the toughening in HA-40 vol.% Ti composite is partly due to crack deflection and mostly due to crack bridging at sites of Ti particles.

3.2. Biological properties of HA-40 vol.% Ti composite

The growing status of new bones in defective bone region around the implants after the implantation of different time was observed by SEM as shown in Fig. 5. After two weeks of the implantation, there were also crannies between bone and implants, especially for pure Ti samples (Fig. 5(a)). However, DB region around the composite was partially filled with new bones (Fig. 5(b)). After four weeks of the implantation, the contacting growth of new bones with Ti implants had not come into being and some narrow crannies still existed (Fig. 5(c)). It could be found from Fig. 5(d) that new bone tissues around the composite began to be mineralized and contacted directly with the composite. After three months of the implantation, the contacting growth of new bones with Ti implants appeared as shown in Fig. 5(e). New bone tissues were maturer than those of four

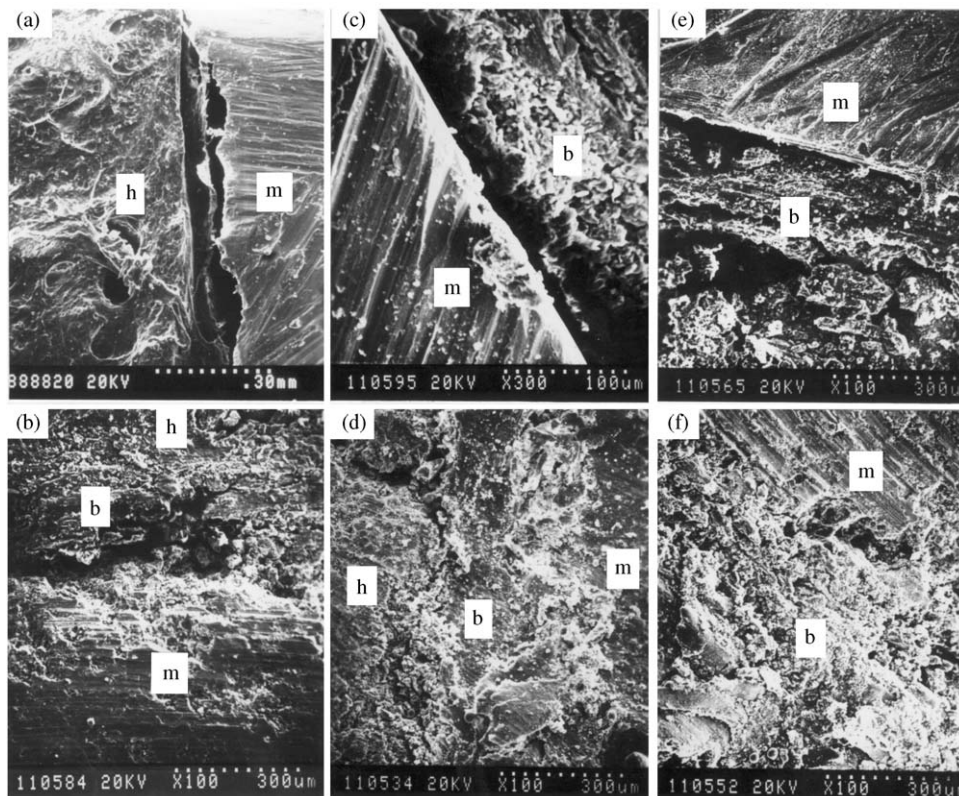


Figure 5 Growing status of new bones in defective bone region around the implants after the implantation of different time observed by SEM. (a) Pure Ti, two weeks; (b) HA-40 vol.% Ti composite, two weeks; (c) pure Ti, four weeks; (d) HA-40 vol.% Ti composite, four weeks; (e) pure Ti, three months; (f) HA-40 vol.% Ti composite, three months. m, implant; b, newborn bone; h, host bone.

weeks and began to transform into laminar bones. The bonding interface between the composite and new bones could not already be distinguished as shown in Fig. 5(f).

The interfacial morphology between the implant and newborn bone after the implantation of different time was observed by light microscopic after stained with HE as shown in Fig. 6. After two weeks of the implantation, more immature newborn osteoid could be found in DB regions for HA–40 vol. % Ti composite implant than those for pure Ti implant as shown in Fig. 6(a) and (b). After four weeks of the implantation, there are some fibrous tissues existing at the partial interface between pure Ti implant and newborn bone (Fig. 6(c)). However, the majority of the composite implant could contact with newborn bone directly and the composite implant was integrated with newborn bone as shown in Fig. 6(d). As shown in Fig. 6(e) and (f), the full osteointegration with newborn bone tissues could be attained for both the composite and pure Ti implants after three months of the implantation.

The experimental results show that HA–40 vol. % Ti composite has excellent biocompatibility. Newborn bones between host bones and the composite implant grew actively and had a growing trend from the brim of host bones to the implants, which indicates that no defensive reaction to the composite implant appears for body tissues and cells. Moreover, the composite implants have no bad effect on the restoring reaction of body tissues and can promote the development of reborn bones. Compared with pure Ti, the composite with excellent biocompatibility has a better affinity to body tissues. The composite implant could integrate with bone. No fibrous tissues came into being at the interface

between the composite implants and new bones during the period after the implants were implanted into the hard tissues. After three months of the implantation, the bonding interface between the composite and new bones could not be distinguished.

4. Conclusions

Based on our previous work, HA–40 vol. % Ti composite with the porosity of 6.7% was fabricated by the optimal technical condition of hot-pressing technique. HA and Ti phases are the predominant phases for the composites like HA–20 vol. % Ti composite. In addition, the sintering process at a high temperature resulted in the formation of two second phases by the decomposition of HA phase, such as $\alpha - \text{Ca}_3(\text{PO}_4)_2$ (TCP) and $\text{Ca}_4\text{O}(\text{PO}_4)_2$.

Comparing with HA–20 vol. % Ti composite manufactured under the same conditions, HA–40 vol. % Ti composite with similar elastic modulus (79.3 GPa) and Vicker's hardness (2.94 GPa) has a higher bending strength (92.1 MPa). Moreover, fracture toughness of HA–40 vol. % Ti composite with crack bridging at sites of Ti particles as the chief toughening mechanisms can reach 2.692 MPa m^{-1} , which is greatly higher than that of HA–20 vol. % Ti composite (0.987 MPa m^{-1}) and can meet the basic toughness demand of the replaced hard tissues for heavy load-bearing applications. Work of fracture of HA–40 vol. % Ti composite with relatively higher fracture toughness and low elastic modulus can reach 91.2 J m^2 , which is 22.9 times that of pure HA ceramic and even 2.4 times that of Al_2O_3 bioceramic (38 J m^2).

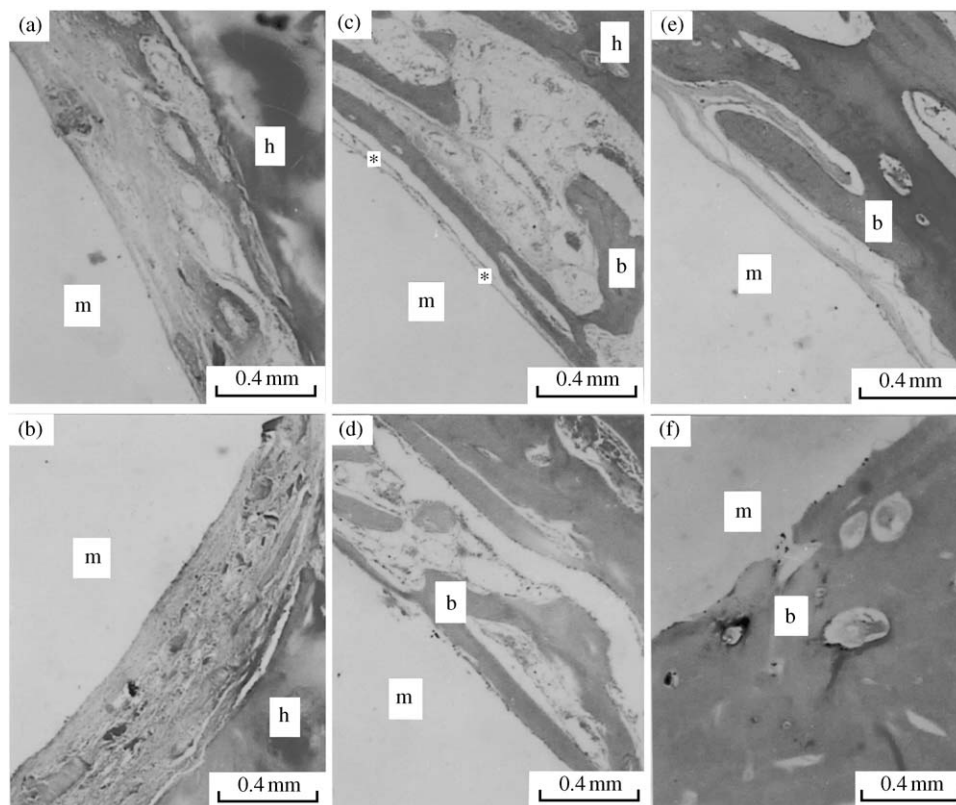


Figure 6 Interfacial morphology between the implant and newborn bone after the implantation of different time observed by light microscope after staining with HE. (a) Pure Ti, two weeks; (b) HA–40 vol. % Ti composite, two weeks; (c) pure Ti, four weeks; (d) HA–40 vol. % Ti composite, four weeks; (e) pure Ti, three months; (f) HA–40 vol. % Ti composite, three months. m, implant; b, newborn bone; h, host bone; *, fibrous tissue.

The results of *in vivo* studies show that HA–40 vol. % Ti composite has excellent biocompatibility and could integrate with bone. No fibrous tissues came into being at the interface between the composite implant and new-born bones. In the early stage after the implantation of the samples, the osteointegration ability of the composite is better than that of pure Ti.

Acknowledgment

The authors are grateful to Prof. S. Z. Xing, Department of Oral and Maxillofacial Surgery, Stomatological Hospital, Nanjing Medical University, for his kind help in part of the experimental work.

References

1. L. L. HENCH, *J. Am. Ceram. Soc.* **74** (1991) 1487.
2. D. F. WILLIAMS, *Mater. Sci. Technol.* **3** (1987) 797.
3. W. SUCHANEK and M. YOSHIMURA, *J. Mater. Res.* **13** (1998) 94.
4. W. BONFIELD, in “Bioceramics: Materials Characteristics vs *In Vivo* Behavior”, Vol. 523, edited by P. Ducheyne and J. E. Lemons (Annals of New York Academy of Science, New York, 1988) p. 173.
5. A. J. RUYSS, A. BRANDWOOD, B. K. MILTHORPE, M. R. DICKSON, K. A. ZEIGLER and C. C. SORRELL, *J. Mater. Sci.: Mater. Med.* **6** (1995) 297.
6. W. SUCHANCK, M. YASHIMA, M. KAKIHANA and M. YOSHIMURA, *J. Am. Ceram. Soc.* **80** (1997) 2805.

7. G. DE WITH and A. J. CORBIJN, *J. Mater. Sci.* **24** (1989) 3411.
8. B. T. MOSSMAN, J. BIGNON, M. CORN, A. SEATON and J. B. L. GEE, *Science* **247** (1990) 294.
9. J. D. BIRCHALL, D. R. STANLEY, M. J. MOCKFORD, G. H. PIGOTT and P. J. PINTO, *J. Mater. Sci. Lett.* **7** (1988) 350.
10. X. ZHANG, G. H. M. GUBBELS, R. A. TERPSTRA and R. METSELAAR, *J. Mater. Sci.* **32** (1997) 235.
11. T. K. CHAKI and P. E. WANG, *J. Mater. Sci.: Mater. Med.* **5** (1994) 533.
12. M. TAKAGI, M. MOCHIDA, N. UCHIDA, K. SAITO and K. UEMATSU, *ibid.* **3** (1992) 199.
13. Y. FANG, D. M. ROY, J. CHENG, R. ROY and D. K. AGRAWAL, *Ceram. Trans.* **36** (1993) 397.
14. J. LI, B. FARTASH and L. HERMANSSON, *Interceram.* **39** (1990) 20.
15. H. Y. JUANG and M. H. HON, *Mater. Sci. Eng.* **C2** (1994) 77.
16. T. NOMA, N. SHOJI, S. WADA and T. SUZUKI, *J. Ceram. Soc. Jpn* **100** (1992) 1175.
17. R. VAN NOORT, *J. Mater. Sci.* **22** (1987) 3801.
18. K. WANG, *Mater. Sci. Eng. A* **213** (1996) 134.
19. C. CHU, P. LIN, Y. DONG, X. XUE, J. ZHU and Z. YIN, *J. Mater. Sci.: Mater. Med.* **13** (2002) 985.
20. P. E. WANG and T. K. CHAKI, *ibid.* **4** (1993) 150.
21. C. L. CHU, J. C. ZHU, Z. D. YIN and S. D. WANG, *Funct. Mater.* **30** (1999) 606.
22. D. M. LIU, *J. Mater. Sci.: Mater. Med.* **8** (1997) 227.
23. I. H. ARITA, V. M. CASTANO and D. S. WILKINSON, *ibid.* **6** (1995) 19.
24. K. T. FABER and A. G. EVANS, *Acta. Metall.* **31** (1983) 565.

*Received 15 April
and accepted 3 December 2003*